ARTICLES

Off-shell effects for the reaction $pp \to \pi d$ at high energies

M. Batinić,[2] T.-S. H. Lee,[3] M. P. Locher,[1] Yang Lu,[1] and A. Švarc[2]

[1] *Paul Scherrer Institute, CH-5232 Villigen PSI, Switzerland*

[2] *Rudjer Bošković Institute, P.O. Box 1016, 41001 Zagreb, Croatia*

[3] *Argonne National Laboratory, Argonne, Illinois 60439*

The reaction $pp \to \pi d$ is studied in a relativistic meson rescattering model. For $1.3 < T_p < 2.4$ GeV the differential cross section and the asymmetry are calculated and compared to experiment. The model introduces simple form factors for the leading πN partial waves which depend on the virtuality of the exchanged mesons, π and ρ. All remaining input is derived from experimental constraints. The data can be described by energy-independent form factors. The asymmetries are sensitive to pp distortion factors and further details of the model.

PACS number(s): 13.75.Cs, 13.85.Fb, 25.10.+s, 25.40.Qa

I. INTRODUCTION

We are studying the reaction $pp \to \pi^+ d$ in the energy range $1.3 < T_p < 2.4$ GeV where good data on cross sections and asymmetries have become available recently [1]. Pion production has been studied earlier in the Δ energy range where an almost complete set of spin observables has been determined experimentally. Extensive calculations in the frame of coupled channel formalisms [2] and in relativistic effective perturbation theory [3,4] have been confronted with the data. The description is in general good, with the exception of notoriously sensitive quantities like the asymmetry A_{y0} and the vector polarization it_{11}. At Δ energies pion rescattering is the dominating physical mechanism as is visible from the energy dependence of the cross section, which clearly displays the resonance. Single nucleon exchange is fairly small in the Δ resonance regime and entirely negligible for the multi-GeV range considered here.

We shall extend the relativistic rescattering model of [3] to the GeV range. At these energies many πN resonances exist as reflected by the well-measured total and differential πN cross sections. The two body nature of the reaction $pp \to \pi^+ d$ forces medium large-momentum transfers onto the deuteron vertex and requires fairly large virtualities of the exchanged meson and nucleon. In [3,4] a Rarita-Schwinger formalism has been used off the mass shell for the Δ resonance. For the higher πN partial waves a simple off-shell recipe consisted of continuing the projectors and equating the partial wave amplitudes off and on the mass shell. At the higher energies which are considered here a special field theoretic description of each of the many πN resonances is not feasible. In this paper we shall introduce simple effective off-shell form factors for the dominating partial waves with parameters derived from data.

In Sec. II we describe the model and the sources of input. Section III gives the results of the basic model and some of its variations while Sec. IV contains a summary.

II. THE MODEL

A. Helicity amplitudes from meson rescattering

The pion rescattering diagram of Fig. 1 corresponds to the amplitudes [3,4]

$$M^{\lambda_d,\lambda_1,\lambda_2} = \frac{-i}{(2\pi)^4} \int d^4\eta \bar{v}(p_2,\lambda_2)\gamma_5 \frac{1}{(p_2-\eta)^2 - m_\pi^2} V_{\pi NN} \frac{-\slashed{\eta}+m}{\eta^2-m^2}[\slashed{\varepsilon}G_a + (\eta \cdot \varepsilon)G_b]$$

$$\times \frac{\slashed{d}-\slashed{\eta}+m}{(d-\eta)^2-m^2}(A+\slashed{q}B)u(p_1,\lambda_1) , \tag{1}$$

where $\lambda_d, \lambda_1, \lambda_2$ are the deuteron and proton helicities and the four vectors are defined in Fig. 1. The pion and nucleon masses are denoted by m_π and m, respectively. The πN invariant amplitudes A and B, the pion vertex function $V_{\pi NN}$ and the deuteron vertex functions $G_{a,b}$ are described below. The relation to the c.m. cross section is

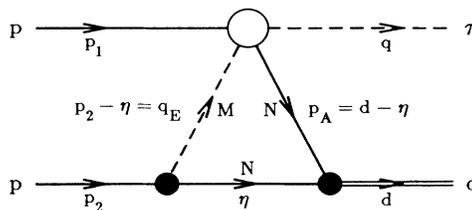$$\frac{d\sigma}{d\Omega} = \left(\frac{m}{4\pi\sqrt{s}}\right)^2 \frac{k}{p}\frac{1}{4}\Sigma \tag{2}$$

FIG. 1. The meson rescattering diagram.

<u>50</u>   1300

TABLE I. Kinematic ranges at $T_p = 0.578$ GeV for $s_{\pi N}$ (GeV^2), $t_{\pi N}$ (GeV^2), x, and x_N (dimensionless) in the coplanar approximation as a function of the loop three-momentum $|\eta|$ and the external angle θ. See Eqs. (4)–(11). Note that $s_{\pi N}$ and x_N are independent of θ in the coplanar approximation. The cutoff loop momentum $|\eta_{\mathrm{cut}}| = 0.367$ GeV is defined preceding Eq. (4).

	Indep. of θ		$\theta = 0$		$\theta = \pi/2$		$\theta = \pi$	
$|\eta|$	$s_{\pi N}$	x_N	x	$t_{\pi N}$	x	$t_{\pi N}$	x	$t_{\pi N}$
0.0	1.459	0.969	−13.9	−0.529	−13.9	−0.303	−13.9	−0.077
$|\eta_{\mathrm{cut}}|/2$	1.383	0.983	−5.5	−0.287	−16.0	−0.252	−26.5	−0.218
$|\eta_{\mathrm{cut}}|$	1.162	0.853	−1.1	−0.100	−22.1	−0.257	−43.0	−0.413

where

$$\Sigma = \sum_{\lambda_d, \lambda_1, \lambda_2} |M^{S}_{\lambda_d, \lambda_1, \lambda_2}|^2 \qquad (3)$$

and the amplitude $M^{S}_{\lambda_d, \lambda_1, \lambda_2}$ is symmetrized in the proton labels. The momenta k and p are defined in Eq. (5) below. For the spin observables and further details see [3].

The energy integration in Eq. (1) is discussed in [3]. The propagator singularities lead to three contributions. The first one corresponds to the spectator contribution where the nucleon η is on shell, the *relativistic impulse approximation*. The pion propagator and the second nucleon propagator lead to antiparticle contributions which have been evaluated in [3] and found to be small. In this paper, as in [4], we shall retain only the relativistic impulse approximation. The remaining three-dimensional integral is calculated numerically using the following input.

B. The deuteron vertex functions

For the deuteron vertex functions we use the invariant expansion from the formalism in [5]. In [6] the S-state and D-state form factors have been fitted separately to modern electron scattering data on the deuteron for momentum transfers up to 2.5 (GeV/c)^2. The vertex functions from [6] are therefore rather directly constrained by accurate data. In these fits certain relativistic corrections [7] and additional vertex functions arising when the second nucleon is off-mass shell [8] are not included explicitly. The vertex functions deduced therefore include these effects effectively.

C. The invariant πN amplitudes off the mass shell

The πN invariant amplitudes A and B are constructed from the Karlsruhe-Helsinki partial waves [9]. It will be necessary to define an off-mass shell extrapolation. It is important to note that the virtualities imposed by the two body kinematics are large. Table I shows the virtualities for the meson, $x = q_E^2/m_\pi^2$, and the nucleon, $x_N = p_A^2/m^2$, for the Δ resonance regime, while Table II shows the kinematics at $T_p = 2.0$ GeV. In defining the transition operator in Eq. (1) we have chosen the explicit form $A + \not{q}B$ for the operator representing the πN amplitudes, which ignores additional operators occurring when one nucleon and one pion are off the mass shell. Replacing the usual definition $(q + q_E)/2$ by q is equivalent for on-shell πN scattering. The choice in Eq. (1) has proven successful for the analysis of continuum pion production in pp scattering [10], which tests the dependence on the virtuality of the exchanged pion. Since the nucleon p_A is not far from its mass shell (see Tables I and II), we shall discard additional operators as in [3,4]. As in the case of the deuteron vertex functions of Sec. II B the πN off-shell form factors introduced further below must therefore be considered as effective form factors. The integral in Eq. (1) converges well due to the presence of the vertex functions. However, when doing the loop integration over $|\eta|$ we shall restrict the three momenta further to $0 \le |\eta| \le |\eta_{\mathrm{cut}}|$, corresponding to $(\sqrt{s} - m)^2 \ge s_{\pi N} \ge (m + m_\pi)^2$. Note that large loop momenta correspond to deeply unphysical πN energies. Subthreshold πN contributions have been discussed and evaluated in [3] for the Δ energy range and found to be of order 20% in the leading amplitudes. Even at resonance the extrapolation of the πN amplitude to subthreshold energies on the scales required becomes unreliable very quickly [9]. Avoiding ill-defined input we therefore re-

TABLE II. Kinematic ranges for $s_{\pi N}$, $t_{\pi N}$, x, and x_N at $T_p = 2.0$ GeV and $|\eta_{\mathrm{cut}}| = 0.895$ GeV/c. See Table I for further notation.

	Indep. of θ		$\theta = 0$		$\theta = \pi/2$		$\theta = \pi$	
$|\eta|$	$s_{\pi N}$	x_N	x	$t_{\pi N}$	x	$t_{\pi N}$	x	$t_{\pi N}$
0.0	3.094	0.737	−42.3	−2.654	−42.3	−1.325	−42.3	0.004
$|\eta_{\mathrm{cut}}|/2$	2.548	0.974	−9.67	−1.305	−57.3	−0.842	−105	−0.380
$|\eta_{\mathrm{cut}}|$	1.162	0.507	−0.15	−0.158	−95.3	−0.562	−191	−0.966

strict the integration to physical πN energies as in [4] where at least the on-shell amplitudes are known reliably. The explicit kinematic dependence of the πN variables can be seen from[1]

$$s_{\pi N} = (p_1 + q_E)^2 = (2E - \eta_0)^2 - \boldsymbol{\eta}^2 , \qquad (4)$$

$$u_{\pi N} = (p_1 - q)^2 = m_\pi^2 + m^2 - 2EE_\pi + 2kp\cos\theta , \quad (5)$$

$$t_{\pi N} = (p_1 - p_A)^2 . \qquad (6)$$

Note that $\eta_0 = \sqrt{\boldsymbol{\eta}^2 + m^2}$ in the impulse approximation. We work in the overall c.m. with total energy $2E$ and external pion scattering angle θ. The three momenta of the external pion and proton are k and p, respectively. The virtualities of the meson and nucleon are

$$x = \frac{q_E^2}{m_\pi^2} = \frac{1}{m_\pi^2}(m^2 + \eta^2 - 2E\eta_0 - 2p|\boldsymbol{\eta}|\cos\theta_\eta) \qquad (7)$$

and

$$x_N = \frac{p_A^2}{m^2} = \frac{1}{m^2}[m_d^2 + \eta^2 - 2E_d\eta_0$$
$$-2|\boldsymbol{\eta}|k(\sin\theta\sin\theta_\eta\cos\phi_\eta + \cos\theta\cos\theta_\eta)] , \quad (8)$$

respectively. Recall that $\eta^2 = m^2$ in the impulse approximation. In Tables I and II we have frozen the loop angles for the purpose of illustration in the coplanar approximation

$$\theta_\eta = \pi - \theta ,$$
$$\phi_\eta = \pi . \qquad (9)$$

which has been shown to be a good approximation for the integral at the Δ resonance [3]. In this approximation,

the virtualities of the meson and nucleon are simplified to

$$x = \frac{q_E^2}{m_\pi^2} = \frac{2}{m_\pi^2}(m^2 - E\eta_0 + p|\boldsymbol{\eta}|\cos\theta) \qquad (10)$$

and

$$x_N = \frac{p_A^2}{m^2} = \frac{1}{m^2}(m_d^2 + m^2 - 2E_d\eta_0 + 2|\boldsymbol{\eta}|k) . \qquad (11)$$

In the actual evaluation we shall not make any such approximation. In [3,4] analytic techniques and a factorization approximation reduced the evaluation of the amplitudes to one-dimensional numerical integration. Modern computers allow one to do the three-dimensional integral over η completely numerically. At the same time the Dirac algebra corresponding to Eq. (1) has now been done on the computer. The results of [3] for the amplitudes have been reproduced to better than 5% for the same input. For the present code a set of amplitudes for six scattering angles at one energy takes 2 min of CPU time on a VAX6630. We thus have an efficient basis for studying variation of the input. In particular the present paper extensively explores different prescriptions for the off-shell behavior of the meson rescattering amplitudes. We work with explicit spinors on the level of helicity amplitudes as in [3], which is by far the most effective way for calculating any desired spin observables.

For the GeV range the following procedure has been implemented to define the off-mass-shell extrapolations for *all* partial waves (contrary to [3] where the 1^+ and 2^- waves have been treated differently). The projectors in the πN partial wave expansion for the invariant amplitudes are calculated with full off-shell kinematics while the partial waves $T_{l\pm}(s_{\pi N})$ are identified off and on the mass shell with $s_{\pi N}$ from Eq. (4)

$$A(s_{\pi N}, t_{\pi N}, x, x_N) = -\frac{4\pi}{q_{\text{c.m.}}^3}\sum_{l\geq 0} T_{l+}^{\text{on}} F_{l+}(x, x_N)[-(E_A + m)(\sqrt{s_{\pi N}} - m)P_l'(\cos\tilde\theta) - (E_A - m)(\sqrt{s_{\pi N}} + m)P_{l+1}'(\cos\tilde\theta)]$$
$$-\frac{4\pi}{q_{\text{c.m.}}^3}\sum_{l\geq 1} T_{l-}^{\text{on}} F_{l-}(x, x_N)[(E_A + m)(\sqrt{s_{\pi N}} - m)P_l'(\cos\tilde\theta) + (E_A - m)(\sqrt{s_{\pi N}} + m)P_{l-1}'(\cos\tilde\theta)] , \qquad (12)$$

$$B(s_{\pi N}, t_{\pi N}, x, x_N) = -\frac{4\pi}{q_{\text{c.m.}}^3}\sum_{l\geq 0} T_{l+}^{\text{on}} F_{l+}(x, x_N)[(E_A + m)P_l'(\cos\tilde\theta) - (E_A - m)P_{l+1}'(\cos\tilde\theta)]$$
$$+\frac{4\pi}{q_{\text{c.m.}}^3}\sum_{l\geq 1} T_{l-}^{\text{on}} F_{l-}(x, x_N)[(E_A + m)P_l'(\cos\tilde\theta) - (E_A - m)P_{l-1}'(\cos\tilde\theta)] , \qquad (13)$$

where $q_{\text{c.m.}}$ is the modulus of the *final*[2] state three-momentum $|\mathbf{p}_f|$ in πN c.m.; see Eq. (15) below. $E_A = \sqrt{q_{\text{c.m.}}^2 + p_A^2}$ is the c.m. energy of the final nucleon calculated from the virtual mass $\sqrt{p_A^2}$ and $\tilde\theta$ is the c.m. off-

shell πN scattering angle. The kinematical variables in the off-shell c.m. of πN are

$$|\mathbf{p}_i|^2 = \frac{(s_{\pi N} + m^2 - q_E^2)^2}{4s_{\pi N}} - m^2 , \qquad (14)$$

$$|\mathbf{p}_f|^2 = \frac{(s_{\pi N} + p_A^2 - m_\pi^2)^2}{4s_{\pi N}} - p_A^2 , \qquad (15)$$

$$\cos\tilde\theta = \frac{2E_N(\sqrt{s_{\pi N}} - E_\pi) + t_{\pi N} - m_N^2 - p_A^2}{2|\mathbf{p}_i||\mathbf{p}_f|} , \qquad (16)$$

---

[1]The definitions of $t_{\pi N}$ and $u_{\pi N}$ in [3] have to be interchanged.

[2]In the calculation [3] the final state momentum has been used as well, contrary to the text in its Appendix.

where $E_N = \sqrt{|\mathbf{p}_i|^2 + m^2}$ and $E_\pi = \sqrt{|\mathbf{p}_f|^2 + m_\pi^2}$.

In the approach of [3] the off-shell definition of the invariant amplitudes A and B was completed by setting $F_{l\pm}(x, x_N) = 1$ for waves higher than 2^- while the 1^+ and 2^- waves were calculated from the Rarita-Schwinger formalism. In the present paper we introduce a Lorentzian form factor for each partial wave. In the simplest version $F_{l\pm}$ will depend only on the meson virtuality x and not on the nucleon virtuality x_N

$$F_{l\pm}(x) = \frac{1 + a_{l\pm}^2}{1 + \left(a_{l\pm} - \frac{1-x}{\Delta_{l\pm}}\right)^2} . \qquad (17)$$

This form guarantees damping for large x and allows rising or falling form factors for $x \leq 1$. The lowest four partial waves get separate form factors while a common factor is used for partial waves higher than 2^-.

At the pion absorption vertex, a Ferrari-Selleri form factor with range parameter ω is introduced,

$$V_{\pi NN} = g(m_\pi^2 - \omega^2)/(q_E^2 - \omega^2) , \qquad (18)$$

with $g^2/4\pi = 14.28$. The range parameter will be fitted. It is the parameter which essentially controls the size of the cross section.

D. Distortion factors

To complete the description of the model we briefly describe the Sopkovich distortion factors [11] which represent higher order rescattering diagrams [12]. The helicity amplitudes of Eq. (1) are replaced by

$$M^J \to \sqrt{S_i^J} M^J \sqrt{S_f^J} . \qquad (19)$$

For each J an L-S decomposition is implicit; for details see the Appendix of [3]. For $J \leq 7$ the projections M^J are calculated numerically. Higher waves remain unchanged. At resonance [3] pion distortion is the dominant effect. As the elastic πd cross section falls steeply with energy, πd distortion gets correspondingly less important in the GeV region. For our energies we have calculated πd phases from the full spin relativistic impulse approximation developed in [13]. At $T_\pi \approx 300$ MeV these phases match the Faddeev calculations from [14]; compare also [2]. The pp distortion reduces the size of the $pp \to \pi d$ cross section considerably at the energies considered here. The *shapes* of the $pp \to \pi d$ cross section and asymmetry are less sensitive. The information on pp amplitudes and phases is far from complete in the T_p range of 1 to 3 GeV. To test the sensitivity we have used two rather different sets of pp amplitudes. In one set we have calculated pp phases ourselves from the coupled channels formalism [15]. In the second set the phases are taken from the direct VPI phase shift analysis [16]. For the purpose of illustration the pp cross section at $T_p = 1.3$ GeV for these two sets are shown in Fig. 2. For ener-
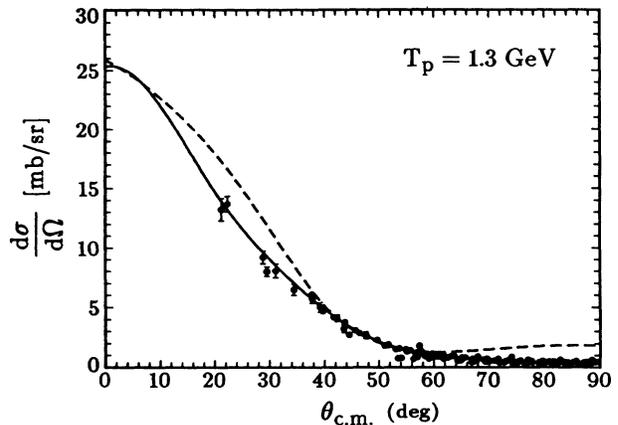

FIG. 2. Elastic pp differential cross section at $T_p = 1.3$ GeV. The dashed line is from the coupled channels calculation [15] and the solid line is from the VPI phase shift analysis [16]. Experimental data are taken from the VPI compilation [16].

gies 1.7 GeV and higher, the forward pp cross sections for the theoretical phases corresponding to [15] are too big. However, since the inelasticities in the two sets of pp phases are comparable, no significant changes are observed in the $pp \to \pi d$ cross sections (compare Fig. 3). Even for the asymmetries pp distortion is not as important as one could expect. We have also calculated all the other spin observables (not shown) and found a sensitivity similar to that of the asymmetry. For the asymmetries in $pp \to \pi d$ the phases calculated from coupled channels [15] do slightly better; see Fig. 3.

III. RESULTS

A. Energy-independent fit

In this section we show a fit to the data at six energies using energy independent form factors. Figure 3 shows the fit for cross sections and asymmetries. Table III shows the parameters for the form factors $F(x)$, Eq. (17), where $\omega^2 = 0.57$ GeV^2. The four lowest waves have been fitted separately; the higher waves (h) from the $2+$ wave up have been fitted with a common form factor. The fit requires only a weak x dependence for these higher waves. Including the vertex range parameter ω in Eq. (18), the total number of parameters is 11. A MINUIT search in this parameter space converges in about 2 h of CPU time. The meson M in Fig. 1 stands not only for π^+ and π^0 exchange, but also for ρ exchange since the leading operator in the nonrelativistic limit differs only by a sign. The form factors Eqs. (17) and (18) represent these meson exchange diagrams effectively. Overall, the calculated cross sections of Fig. 3 describe the data quite well. At 1.88 and 2.1 GeV the calculation shows slightly too much forward dipping, while at 1.3 GeV the cross section is too flat with respect to modern data [1]. These deviations may be due to the presence of fairly strong resonances at these energies which are not well described
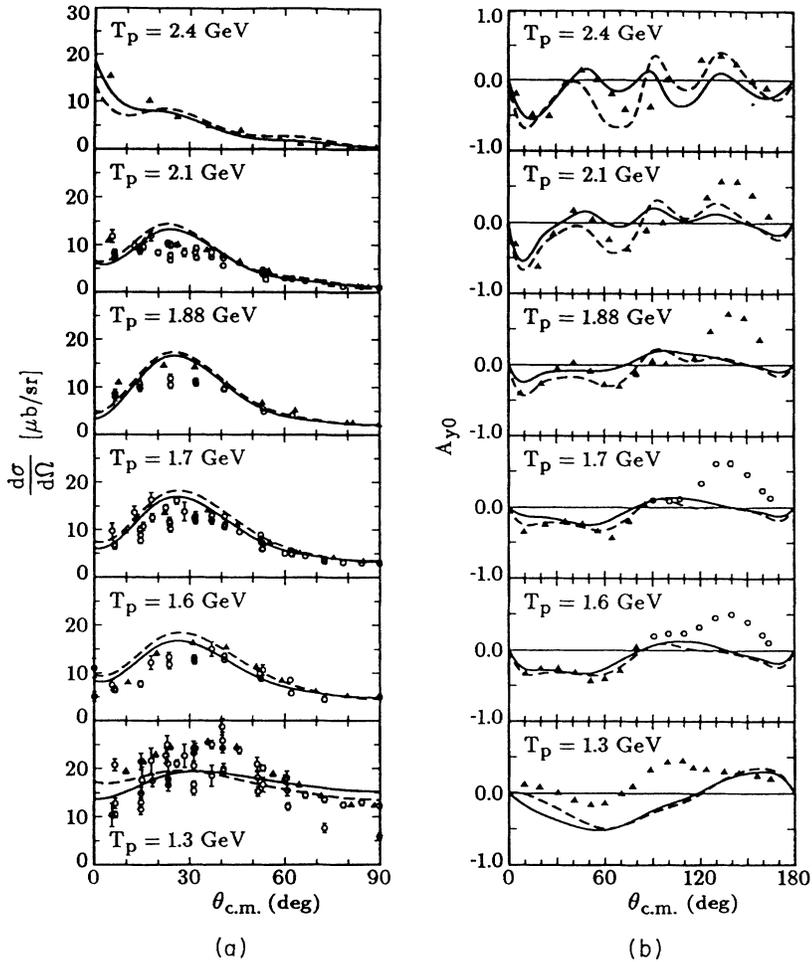
FIG. 3. Energy *independent* analysis: (a) The c.m. differential cross section for $pp \to \pi d$ as a function of the proton kinetic lab energy T_p. (b) The asymmetry parameter. The data from the recent Saclay measurement [1] are indicated by solid triangles while previous measurements at nearby energies [19,20] are indicated by open circles. The dashed curves are for the pp distortion factors from the coupled channel model [15] while the the solid curves are the results for the pp phase shifts from VPI [16]. See Table III for the parameters of the fit.

by average form factors; compare Sec. III D below.

The asymmetries are also described surprisingly well. Note that the calculation is including distortion factors for the initial pp and final πd states (see Sec. II D). In the GeV range πd distortion is not important (in contrast to the Δ resonance range). The pp distortion affects mostly the overall size of the cross section. Remaining sensitivities are illustrated by the solid and dashed lines. The solid lines contain pp phases from [16], while the dashed lines use pp phase shifts which have been calculated from the coupled channel formalism [15] for the present purpose. The backward peak seen in the asymmetries at medium energies does not seem to be related to ambiguities in the distortion factors.

B. Energy-dependent analysis

Using the procedure described above we have also fitted the form factors Eq. (17) for each energy separately. The fit for cross section and asymmetry is shown in Fig. 4. The parameters in Table IV show a fair degree of stability. No simple solution has been found which describes the backward peaks for the asymmetries. The cross section at 1.3 GeV is well described by a moderate change for the 1^+ wave and by a fairly flat form factor (large width Δ_h) for the higher πN partial waves.

C. Alternative parametrizations of form factors

At resonance the Rarita-Schwinger form factors of [3] used for the dominant 1^+ πN wave amount to practically linear form factors both in x and x_N, as we have checked. The 1^+ contribution to the invariant πN amplitudes A and B can thus be approximated by
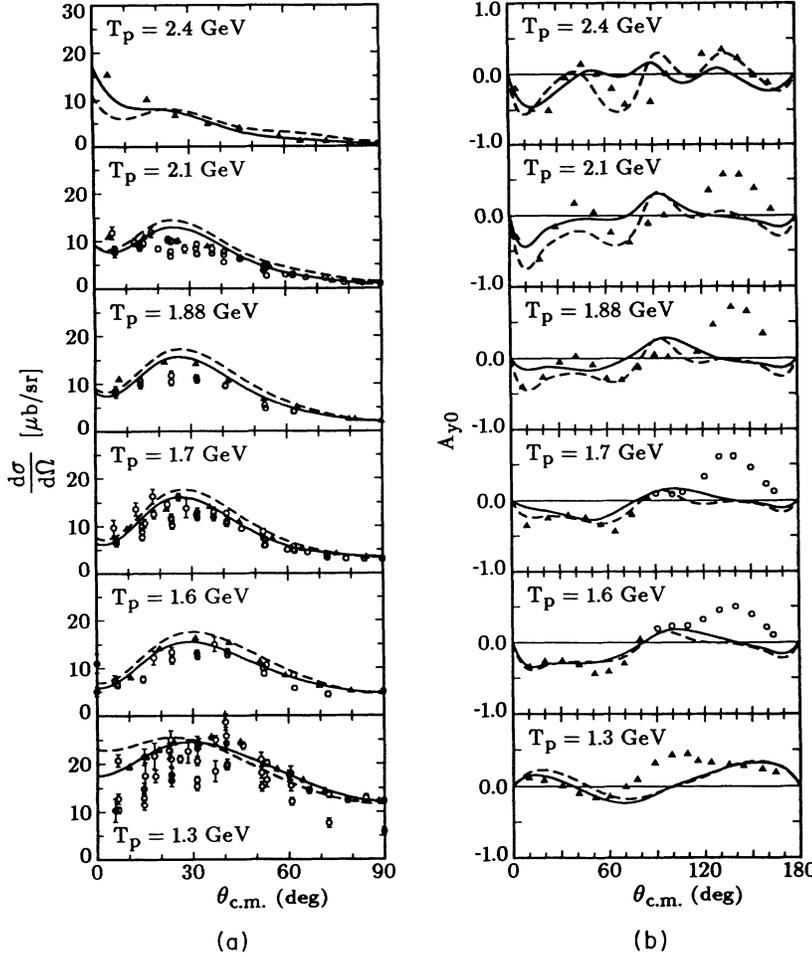
TABLE III. The parameters of the Lorentzian form factors Eq. (17) for the πN partial waves from the energy *independent* analysis. Note a and Δ are dimensionless.

	0^+	1^-	1^+	2^-	h
a	0.64	0.73	−0.47	0.74	0.4
Δ	7.7	31.4	3.0	14.5	25

FIG. 4. Energy *dependent* analysis. See Fig. 3 for notation and Table IV for the parameters of the fit.

$$A = -\frac{4\pi}{q_{c.m.}^3}T_{1+}^{on}[-(E_A + m)(\sqrt{s_{\pi N}} - m)P_1'(\cos \tilde{\theta})F_0(x, x_N) - (E_A - m)(\sqrt{s_{\pi N}} + m)P_2'(\cos \tilde{\theta})F_1(x, x_N)] , \qquad (20)$$

$$B = -\frac{4\pi}{q_{c.m.}^3}T_{1+}^{on}[(E_A + m)P_1'(\cos \tilde{\theta})F_0(x, x_N) - (E_A - m)P_2'(\cos \tilde{\theta})F_1(x, x_N)] , \qquad (21)$$

where

$$F_0(x, x_N) = f_0(x)f_0^N(x_N) \qquad (22)$$

with a similar expression for $F_1(x, x_N)$. The functions f_i

are linear $(i = 0, 1)$:

$$f_i(x) = a_i + (1 - a_i)x , \qquad (23)$$

$$f_i^N(x_N) = a_i^N + (1 - a_i^N)x_N . \qquad (24)$$

The same form factors are used for A and B.

The presence of the meson and deuteron vertex functions guarantees convergence of the integral even without

TABLE IV. The parameters of the Lorentzian form factors Eq. (17) for the πN partial waves from the energy *dependent* analysis. Note a and Δ are dimensionless.

| | T_p (GeV) | | | | | |
	1.3	1.6	1.7	1.88	2.1	2.4
ω^2 (GeV^2)	0.65	0.6	0.6	0.6	0.82	0.6
a_{0+}	−0.052	1.05	0.23	1.22	0.89	−1.07
Δ_{0+}	5.0	5.1	14.4	6.64	8.97	28.8
a_{1-}	1.53	1.08	0.98	0.97	0.66	0.77
Δ_{1-}	10.4	15.2	16.8	16.2	22.1	20.8
a_{1+}	−5.0	−0.034	−0.23	0.41	0.30	0.38
Δ_{1+}	4.6	4.0	4.0	4.0	4.0	4.0
a_h	−4.9	1.11	1.43	1.36	0.94	0.34
Δ_h	100	5.0	5.0	5.0	8.03	22.0

TABLE V. Parameters for the linear form factors at $T_p = 0.578$ GeV used in Fig. 5. Both the fit and the linear approximation to the Rarita-Schwinger formalism [3] for the Δ resonance contribution are shown. See Sec. III C for more details.

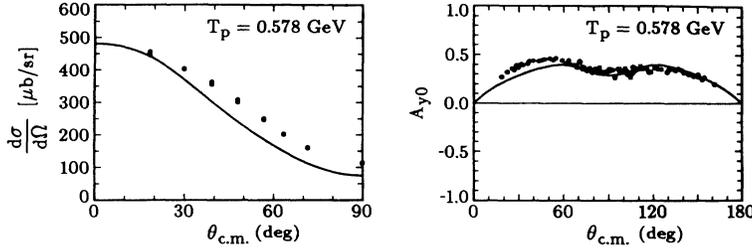|	a_0	a_1	a_0^N	a_1^N
Rarita-Schwinger	1.004	1.04	−1.0	−0.5
Fit	0.948	1.06	−1.68	−1.35

FIG. 5. Differential cross section and asymmetry for $pp \rightarrow \pi d$ at $T_p = 0.578$ GeV with linear form factors. Experimental data are from [21,22]. See Sec. III C.

any cutoff in $|\eta|$. The resulting observables from a minimization of the linear approximation at $T_p = 0.578$ GeV are shown in Fig. 5. The corresponding parameters for the linear form factors are shown in Table V for the free fit where also the linear approximation for the Rarita-Schwinger expression in [3] is shown.

Since the linear approximation reproduces the results of [3] at $T_p = 0.578$ GeV very accurately we have extended this procedure to $T_p = 1.5$ GeV. In this case we use a product of linear vertex functions for all $j = l+$ waves simultaneously and we use the same form factors also for the $j = l-$ waves, generalizing Eqs. (20)–(24). The result from fitting the parameters in Eq. (22) to the cross section and asymmetry at 1.5 GeV are shown in Fig. 6, the corresponding form factors in Table VI. The fit is not convincing. Attempting simultaneous minimization of the remaining energies in the GeV region does not lead to good fits with stable parameters either. We have therefore abandoned this approach. It could of course be too restrictive to use the same form factors for the $j = l+$ and $j = l-$ waves.

We mentioned in the Introduction that many spin observables have been measured in the Δ resonance regime, in particular the Cartesian spin parameters A_{ij}. In [17] a procedure has been formulated which is capable of explaining the finer details of the spin observables. It consists in extrapolating the spin-flip and spin-nonflip parts of the πN amplitudes differently. A difference of 13% for $x \approx -10$ where the integrand peaks, is enough to obtain a very good fit to the data at resonance. This amounts to introducing separate form factors for the invariant amplitudes A and B.

Since the only spin observable measured in the GeV range is the asymmetry we have not introduced this procedure here. Not surprisingly, preliminary tests in the GeV range have shown a fair amount of sensitivity to this degree of freedom.

D. The role of strong local πN resonances

We already noticed the undesirable forward dip in the global fit to the cross sections at $T_p = 2.1$ and 1.88 GeV in Fig. 3 at least in comparison with the recent data from [1]. We have therefore explored the possible role of several πN resonances for the energy $T_p = 2.1$ GeV. We found that the $N(1680) F_{15}$ resonance in particular can affect the cross section significantly. Figure 7 shows the corresponding cross section. For the figure we have replaced in the isospin-1/2 channel the overall form factor F_{3-} in Eqs. (12) and (13) with two separate form factors which multiply the terms containing P_2' and P_3'. On the amplitude level the modification of the forward cross section shown amounts to 50% increase in the P_2' term and 50% decrease in the P_3' term. The result seems to confirm the importance of local resonance effects. In the absence of convincing constraints for all these resonance form factors we refrain, however, from introducing these new parameters into the fit. We must also remember that with increasing energy the πN resonances couple to $\pi\pi N$ states with increasing strength. This is particularly true for $\Delta(1600) P_{33}$, $\Delta(1620) S_{31}$, $\Delta(1700) D_{33}$, $\Delta(1905) F_{35}$, $\Delta(1910) P_{31}$, $\Delta(1950) F_{37}$, $N(1440) P_{11}$, $N(1520) D_{13}$, $N(1675) D_{15}$, $N(1680) F_{15}$, $N(1720) P_{13}$, $N(2190) G_{17}$ [18]. Note that the $\pi\pi N$ and other decay channels are of course reflected in the total πN cross section on shell by the unitarity relation and are thus already partly contained in the normalization of our calculation at each energy. Two-meson exchange diagrams could be introduced into our model explicitly for the price of a considerable number of new parameters. We think this is presently neither practical nor warranted. It is however clear that the form factors of Tables III and IV effectively also represent these effects.
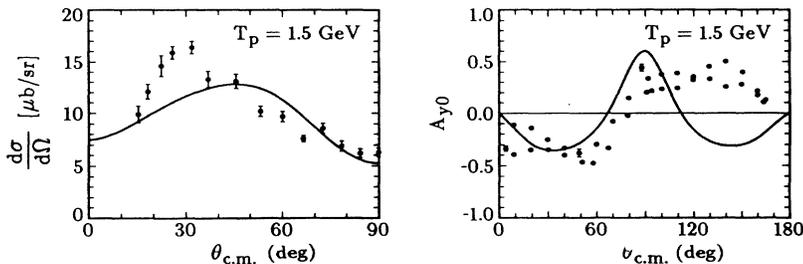

FIG. 6. Differential cross section and asymmetry for $pp \rightarrow \pi d$ at $T_p = 1.5$ GeV with linear form factors. Data are from [20,23]. See Sec. III C.

TABLE VI. Parameters for the form factors at $T_p = 1.5$ GeV from the fit. Compare Sec. III C and Fig. 6.

a_0	a_1	a_0^N	a_1^N
0.974	0.911	−0.30	−1.65

IV. SUMMARY AND CONCLUSION

Our model calculation has shown that meson rescattering is capable of describing the elementary $pp \to \pi d$ reaction also in the GeV range. One of the most important physics ingredients is the off-mass shell behavior of the exchanged mesons. Fairly simple energy-independent effective form factors for the leading meson-nucleon partial waves are able to describe cross sections and asymmetries in a semiquantitative way. The simplest model leading to a global fit contains no explicit form factors for the virtual nucleon. These would represent corrections to the deuteron vertex function and additional off-shell effects for the meson-nucleon amplitude. The deuteron vertex corrections are included effectively in the parametrization used (see Sec. II B) but the importance of the nucleon virtuality x_N in the meson-nucleon amplitude is not known. The spectral function in the nucleon mass variable starts at $m + m_\pi$ and is generally considered to be weak. Moreover, for our process $pp \to \pi d$ the range of x_N is fairly restricted (see Tables I and II). At the Δ resonance (see Sec. III C) a fit to the data requires some x_N dependence, however. Despite that, we believe that
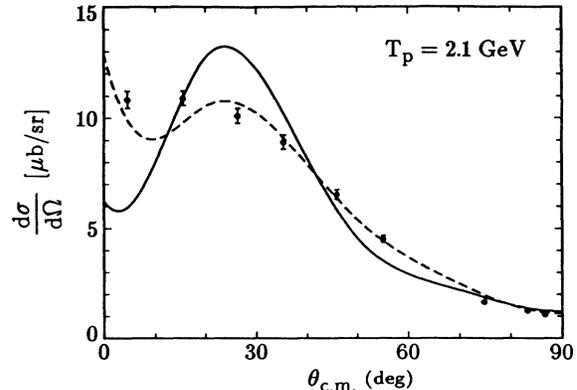

FIG. 7. Differential cross section for $pp \to \pi d$ at $T_p = 2.1$ GeV with resonance effect shown in dashed line. The solid line is the energy independent fit shown in Fig. 3 with VPI pp phases. Data from [1].

the remaining discrepancies in the GeV range considered in this paper are most likely due to the effects of local resonances and the exchange of several pions and further meson resonances beyond the level already present implicitly in our calculation. We also expect that the finer details of the spin observables in the GeV range, which are not measured yet, will require separate extrapolations for the invariant πN amplitudes A and B, as was shown to be necessary [17] in Δ resonance range.

[1] J. Yonnet et al., Nucl. Phys. A562, 352 (1993).

[2] H. Garcilazo and T. Mizutani, πNN Systems (World Scientific, Singapore, 1990).

[3] W. Grein, A. König, P. Kroll, M.P. Locher and A. Švarc, Ann. Phys. (N.Y.) 153, 301 (1984).

[4] M.P. Locher and A. Švarc, J. Phys. G 11, 183 (1985).

[5] M. Gourdin, M. Le Bellac, F.M. Renard, and J. Tran Thanh Van, Nuovo Cimento 37, 524 (1965).

[6] M.P. Locher and A. Švarc, Z. Phys. A 338, 89 (1991); Fiz. 22, 549 (1990).

[7] R.G. Arnold, C.E. Carlson, and F. Gross, Phys. Rev. C 21, 1426 (1980); R.S. Bhalerao and S.A. Gurvitz, Phys. Rev. Lett. 47, 1815 (1981).

[8] F. Gross, Phys. Rev. D 10, 223 (1974).

[9] G. Höhler, in Pion Nucleon Scattering, edited by H. Schopper, Landolt-Börnstein, New Series, Group I, Vol. 9b, Pts. 1 and 2 (Springer-Verlag, Berlin, 1983).

[10] A. König and P. Kroll, Nucl. Phys. A356, 345 (1981).

[11] N.J. Sopkovich, Nuovo Cimento 34, 186 (1962).

[12] L. Durand III and Yam Tsi Chiu, Phys. Rev. 139, B646 (1965).

[13] K. Kubodera and M. P. Locher, Phys. Lett. B87, 169 (1979).

[14] H. Garcilazo, Phys. Rev. Lett. 45, 780 (1980); Phys. Rev. C 35, 1804 (1987) and private communication; N. Girard, C. Fayard, and G.H. Lamot, ibid. 21, 1959 (1980).

[15] T.-S.H. Lee, Phys. Rev. C 29, 195 (1984).

[16] R.A. Arndt, L.D. Roper, R.A. Bryan, R.B. Clark, B.J. VerWest, and P. Signell, Phys. Rev. D 28, 93 (1983); VPI phase shifts for pp are obtained from the SAID program.

[17] M.P. Locher and A. Švarc, Few-Body Systems 5, 59 (1988).

[18] Particle Data Group, K. Hikasa et al., Phys. Rev. D 45, S1 (1992).

[19] M. Akemoto et al., Phys. Lett. 149B, 321 (1984); D. Dekkers, B. Jordan, R. Mermod, C.C. Ting, G. Weber, T.R. Willitts, K. Winter, X. de Bouard, and M. Vivargent, Phys. Lett. 11, 161 (1964); N.W. Reay, A.C. Melissinos, J.T. Reed, T. Yamanouchi, and L.C.L. Tuan, Phys. Rev. 142, 918 (1966).

[20] R.M. Heinz, O.E. Overseth, D.E. Pellett, and M.L. Perl, Phys. Rev. 167, 1232 (1968).

[21] J. Hoftiezer, Ch. Weddingen, P. Chatelain, B. Favier, F. Foroughi, C. Nussbaum, J. Piffaretti, S. Jaccard, and P. Walden, Nucl. Phys. A402, 429 (1983); A412, 286 (1984); J. Hoftiezer, G.S. Mutchler, Ch. Weddingen, J.A. Konter, S. Mango, A. Berdoz, B. Favier, and F. Foroughi, ibid. A412, 273 (1984).

[22] E. Aprile et al., Nucl. Phys. A379, 369 (1982).

[23] R. Bertini et al., Phys. Lett. 162B, 77 (1985); 203B, 18 (1988).